Large Eddy Simulation of pulsatile blood flow

Manosh C. Paul[1] *, Md. Mamun Molla[1], Giles Roditi[2]
[1]Department of Mechanical Engineering, University of Glasgow,
Glasgow G12 8QQ, UK
[2]Department of Radiology, Glasgow Royal Infirmary,
16 Alexandra parade, Glasgow G31 2ER, UK

Abstract

Large Eddy Simulation (LES) is performed to study pulsatile blood flow through a 3D model of arterial stenosis. The model is chosen as a simple channel with a biological type stenosis formed on the top wall. A sinusoidal non-additive type pulsation is assumed at the inlet of the model to generate time dependent oscillating flow in the channel and the Reynolds number of 1200, based on the channel height and the bulk velocity, is chosen in the simulations. We investigate in detail the transition-to-turbulent phenomena of the non-additive pulsatile blood flow downstream of the stenosis. Results show that the high level of flow recirculation associated with complex patterns of transient blood flow have a significant contribution to the generation of the turbulent fluctuations found in the post stenosis region. The importance of using LES in modelling pulsatile blood flow is also assessed in the paper through the prediction of its sub-grid scale contributions. In addition, some important results of the flow physics are achieved from the simulations, these are presented in the paper in terms of blood flow velocity, pressure distribution, vortices, shear stress, turbulent fluctuations and energy spectra, along with their importance to the relevant medical pathophysiology.

Keywords: Pulsatile blood flow, Arterial stenosis, Transition to turbulent, Large Eddy Simulation

*E-mail:m.paul@mech.gla.ac.uk, Tel:+44 (0)141 330 8466, Fax:+44 (0)141 330 4343

1 Introduction

The term arterial stenosis refers to narrowing of an artery where the cross-sectional area of a blood vessel is reduced, this retards blood flow and as a result at high degrees of stenosis flow transients to turbulent with a pressure drop across the stenotic region. The most common cause is atherosclerosis where cholesterol and other lipids are deposited beneath the intima (inner lining) of the arterial wall. As the amount of this fatty material increases there is an accompanying proliferation of connective tissue and the whole forms a thickened area in the vessel wall called plaque.

The alteration in flow dynamics in turn produces abnormal wall shear stress both at the plaque and at the post stenotic area such that the plaque may fissure and rupture exposing the lipid plaque core to the blood stream with potential for thrombosis (blood clotting) at the site of rupture. This development of atherothrombosis may dangerously acutely occlude the vessel with, in critical territories such as the coronary arteries and cerebral vessels, potentially catastrophic results. Non-occlusive atherotrhombosis is also clinically important as the thrombotic material deposited is often unstable and a source of distal embolism, this is particularly important in the extracranial carotid arteries as a source of stroke.

Interestingly, it is the sites of low wall shear stress that are prone to these lipid accumulations and hence plaque formation, Malek *et al* [1], this is thought to be through stimulating an atherogenic phenotype in the cells of the endothelium (vessel lining). Furthermore, it is the pulsatile nature of flow and the oscillatory shear index that is increasingly being recognised as the important factor in this process as has been shown in 4D MRI experiments, see Frydrychowicz *et al* [2].

The blood flow through arteries is inherently unsteady due to the cyclic nature of the heart pump. The obstruction presented by a moderate or severe arterial stenosis can lead to a highly disturbed flow region downstream from the stenosis; the development of transition to turbulent flow in arteries has clinical interest as outlined above. The fluid dynamics of post-stenotic blood flow plays an important role in the diagnosis of arterial disease, for example the quantification of arterial stenosis by both duplex ultrasound and quantitative flow MRI techniques relies on measurements of the flow velocity/acceleration at/beyond the stenotic segment to infer the degree of underlying stenosis. From the point of view of accurate computational modelling, such flow can be challenging.

Giddens and co-workers performed many experiments to measure the velocity and disturbances of turbulent flow through arterial stenosis, see [3; 4]. In addition, most computational studies of laminar to turbulent flow in stenosis in the literature are 2D, e.g. Ghalichi *et al* [5] and Lee *et al* [6] who used Reynolds-average Navier-Stokes (RANS), particularly, k-ω turbulence model. **A recent study of Younis *et al* [7] also shows that the RANS can yield useful predictions for flow in a real stenotic artery.** However, some limitations of using the conventional RANS turbulent models to simulate pulsatile flows are clearly pointed out by Scotti and Piomelli [8]. On the other hand, the Large-Eddy Simulation (LES) approach, which lies between Direct Numerical Simulation (DNS) and RANS, has already proved to be an excellent technique for modelling turbulent flow. In DNS all the

large and small scales are resolved, however, in LES only the large scales, hence the energy-containing scales of turbulence are resolved while the smaller (subgrid) scales (SGS) are modelled. DNS is suitable for a low Reynolds number flow but LES is applicable for small to high Reynolds number flows and requires less time and grid densities than DNS, since in LES the smallest scales need not to be resolved.

With the help of a dynamics subgrid scale model, LES has already proved to be capable of modelling a transition to turbulent pulsatile flow, e.g. see Scotti and Piomelli [8], Mittal *et al* [9; 10], and Liang and Papadakis [11]. However, most previous applications of LES found in the literature have concentrated only on other engineering flows, exceptions to those are Mittal *et al* [9; 10] who used LES to study pulsatile flow in a planar channel with a semi-circular type constriction which, however, does not replicate accurately the formation of a stenosis in an arterial wall. The formation of stenosis in the present model is different than [9; 10]. A smooth constriction, which is generated using the relation given in [3], gives a fairly reasonable representation of a biological arterial stenosis. Furthermore, in most previous works the flow pulsation is usually added with a fully developed mean flow, but it is argued by Pedley [12] that a highly pulsatile flow is not believed to be additive, i.e. non-additive. In this paper we have used the non-additive approach in the pulsation of the blood flow to investigate in detail transition to turbulent phenomena of blood flow downstream of a stenosis by applying a LES technique. Particular attention is given to some of the physical results and their fluid-dynamics roles in causing some of the potential pathological states secondary to stenosis.

2 Computational model

The geometry shown in Fig. 1 consists of a 3D channel with a one sided stenosis on the upper wall centred at $y/L = 0.0$ where y is the horizontal distance or the distance along flow and L is the height of the channel. In the model the height (x) and its width (z) are kept the same which forms a square cross-section at the upstream and downstream of the stenosis. The length of the stenosis is equal to twice that of the channel height, and the stenosis reduces the channel cross-sectional area of 50% and its formation in the model is eccentric. Before the stenosis the channel length is $5L$, and $15L$ is the downstream region of the stenosis.

We assumed that the fluid is homogeneous, incompressible and Newtonian. The governing equations are the 3D Navier-Stokes equations of motion and the mass continuity. From Pedley [13] and Fung [14], it is known that the blood flow in a large vessel can be modelled accurately as a Newtonian fluid, which refers to use the Navier-Stokes equations for investigating the post stenotic flow physics of blood flow through an arterial stenosis. The viscosity of blood is taken as $3.71 \times 10^{-3} m^2 sec^{-1}$ with a mass density of $1.06 \times 10^3 kgm^{-3}$, [5].

In LES a spatial filter is applied to the governing equations to separate the small scale motion from the large scale. The effects of the small scales appearing in the sub-grid scale (SGS) stresses are modelled using the Smagorinsky model [15] , while the large scale motions are resolved fully. In addition, the subgrid dynamic model of Piomelli and Liu [16] is applied to determine the values of the unknown Smagorinsky constant. An inhouse LES code is used to solve the filtered governing equations,

which is second order accurate in both time and space and fully implicit, and has been applied extensively in other engineering flows, for more details see Jones and Wille [17] and the relevant references therein.

No slip boundary conditions are used for the lower and upper walls of the model, and at the outlet a convective boundary condition is used. In the spanwise boundaries, a periodic boundary condition is applied to model the spanwise homogeneous flow. Non-uniform dense meshes are used near the top and bottom walls of the model to capture the thin shear layer developed in the vicinity of the walls. The meshes are concentrated at the region immediate downstream of the stenosis where high vortices generate.

A sinusoidal type fully developed laminar streamwise velocity profile is used at the inlet of the model stenosis, which is formulated as,

$$\bar{v}(x,t) = 6\bar{V}\frac{x}{L}\left(1-\frac{x}{L}\right)\frac{1}{2}\Big[1-\cos\left(\frac{2\pi t}{T}\right)\Big], \tag{1}$$

where $\bar{V}$ is the bulk velocity and T is the time period of the pulsation. The flow gets fully developed in the x-direction while the pulsation takes place in the t-direction with a peak occurring at the middle of every period. In addition, the flow pulsation gets zero at the beginning and end of every cycle and that is why it is referred here as non-additive.

3 Results and discussion

The computational results presented here are with the grid size of $90\times300\times90$ ($x\times y\times z$) and the flow Reynolds numbers of 1200. A grid independent test taking the grid size higher than the above e.g. $120\times350\times90$ is performed to check the appropriate grid density required in LES to resolve the large scale flow. Some results of this test are presented in Figs. 7 in terms of the time-mean streamwise velocity and the wall shear stresses, proving the fact that the grid size of $90\times300\times90$ is well enough for $Re = 1200$ to capture the high level of circulation found in the post-stenosis region. A variable timestep is used at the beginning of the simulations ensuring that the maximum Courant number lies between 0.1 and 0.2. After passing some initial transients the timestep at the order of 10^{-3} is maintained in the simulations for both the grid arrangements.

The contour plot of the dynamic Smagorinsky model constant of the sub-grid scale is presented in Fig. 2. As illustrated in Fig. 2, the value of the Smagorinsky constant is predicted significantly high at immediate downstream of the stenosis because of the turbulent nature of the post-stenotic blood flow. A maximum value of about 0.081 is found in the present model, which is close to 0.1 – a typical value of the Smagorinsky constant usually used for other LES simulations of turbulent channel flow. Before the stenosis the contribution of the model constant is negligible, because at the upstream the blood flow remains laminar. The maximum value of the normalised SGS eddy viscosity, μ_{sgs}/μ, is found about 0.23 in the simulation, which corresponds to the fact that the sub-grid scale model contributes a maximum of 23% extra dissipation into the flow, mainly at the post stenosis region where the transition to turbulent takes place.

Fig. 3 represents the flow field shown at different cross-sectional positions of the post stenosis region using the cross-flow velocity components, $\bar{u}-\bar{w}$. By inspection of these vector plots, obviously, we can conclude that the flow nature after the stenosis is turbulent (also see the energy spectra in Fig. 9). At the centre of the stenosis, at location $y/L = 0$, the flow is transitional; and the separated shear layer from the throat of the stenosis has caused large scale circulations close to the post-lip of the stenosis, at location $y/L = 1$; as a result the wall shear stresses plotted in Fig. 6 are found highly oscillative in this region. In addition, the strength of the flow circulation is found quite large at location $y/L = 2$, which again contributes to the growth of the turbulent fluctuations in the downstream flow (see Fig. 8). However, the intensity of the flow circulations gradually decreases from $y/L = 3$ to 5, and towards the further downstream of the post stenosis (not shown in the figure) it is found that the strength of the circulations diminishes substantially as the effects of the stenosis to the flow reduces there.

In Fig. 4, the spanwise-averaged vorticity (ω) contours are plotted, where a total of 14 unequal contour levels (shown in the colour bar) are chosen between the maximum and minimum values of ω. The dashed contour lines in the figure (colour ranging from green to blue) correspond to the negative values of ω where the vortex cells rotate in the anti-clockwise direction; whereas the solid lines (colour ranging from green to red) are for the positive contours representing the clockwise rotational vortices. Due to the separation of the wall shear layers from the throat of the stenosis, the large recirculation region with a pair of positive and negative vortices is created near $y/L = 1$, revealing the fact that the blood flow is reversed for a significant time in this region which is a potential source of blood-clot in the post stenosis. In addition, from the pathological point of view, this prediction is quite important in such that the flow recirculation usually increases the staying time of blood in the post stenosis that may cause heart attack or brain stroke to a patient with stenoied artery. At the further downstream of the stenosis, the motion of the blood flow becomes very complex, where the pair of vortices breaks down, which in turn causing oscillations in the pressure and shear stress distributions at the post stenosis region (see Figs. 5 and 6).

The instant pressure distributions shown in Fig. 5 are recorded in (a) the upper wall and (b) the lower wall at four different phases of the pulsation starting from its peak at the 9.5th cycle which is denoted by "a" in the figure. The phase denoted by "b" indicates the pulse position of $\frac{1}{4}\pi$ from the peak, while "c" and "d" are for $\frac{2}{4}\pi$ and $\frac{3}{4}\pi$ respectively. The significant level of pressure drops, occurring at the throat of the stenosis while it is extreme when the pulsation attains its peak position "a", is associated with the fact of rising of the streamwise velocity of blood which transients from the throat (see the mean velocity plot in Fig. 7(a)). In addition, the pressure drops are quite large at the upper wall compared with those of the lower wall due to the clear effect of the stenosis located in the upper wall.

In Fig. 6, the wall shear stresses are presented at the peak pulsation (denoted by "a" in the previous figure). In the upper wall, where the stenosis appeared, the large drop in the shear stresses just prior to the centre of the stenosis is caused by the flow separation observed earlier in Fig. 4; while the flow recirculation, also seen in Fig. 4, has contributed in producing the highly oscillative positive and negative

shear stresses close to the post-lip of the stenosis, before $y/L = 2$. However, towards the far downstream region these shear stresses decrease gradually as the intensity of the flow circulation reduces there. On the other hand, the shear stresses in the lower wall initially rise at the centre of the stenosis, followed by a drop to the post-lip at $y/L = 1$, then further rise to $y/L = 2$, and finally become approximately constant towards the far downstream. From the medical point of view, these results of large and oscillative wall shear stresses found in the post stenosis zone could have a quite impact in causing, or influencing to cause, potential damage to the materials of red blood cells (Sutera and Mehrjardi [18]) and also to the endothelium or inner side of post-stenotic blood vessel (Fry [19]).

The time-mean centreline velocity, normalised by the bulk velocity $\bar{V}$, is presented in Fig. 7(a), along with the direct comparison of the results obtained by the two grid configurations, $120 \times 350 \times 90$ and $90 \times 300 \times 90$, used in LES. As clearly seen, this comparison agrees well and is quite satisfactory, which is again proving the fact that the flow resolutions with these two grid arrangements are not so sensitive. In addition, the normalised time-mean wall shear stresses, depicted in Fig. 7(b), also show that for both the grid setups overall their agreements are satisfactory.

The centreline turbulent velocity fluctuations are recorded with time at one post stenotic position, $y/L = 2.0$, and presented in Fig. 8 after normalising with the bulk velocity $\bar{V}$, in order to show clearly the cycle-to-cycle variations of the turbulent velocity fluctuations. As seen in the figure, the magnitude of the velocity fluctuations is recorded high at the middle position of every cycle, because of the pulsatile velocity profile which gets maximum at the mid-cycle location. The corresponding energy spectra, plotted in Fig. 9 against the Strouhal number, $St = (fL/\bar{V})$, of the vortex shedding frequency, f, along with the straight line of $(St)^{-5/3}$, show clearly the presence of the broad band region or the inertia sub-range region of slope $-\frac{5}{3}$ at the post stenotic region, which is providing us with a further confirmation about the turbulent nature of the transient blood flow downstream of the stenosis.

4 Conclusion

A Large Eddy Simulation with the dynamic sub-grid model has been applied to study non-additive pulsatile blood flow in a 3D model of arterial stenosis. To the best of our knowledge, this is the first attempt to study the transition to turbulent blood flow of a non-additive pulsation in a model of biological type arterial stenosis using the LES technique. We have found that the sub-grid model has a remarkable contribution with the resolved scale and it dissipates about 23% energy of the flow when $Re = 1200$, which again justifies the importance of using LES in the modelling of biological type flow.

At the post stenotic region the blood flow transients to turbulent and takes a complex pattern, where both the pressure and shearing stresses take on an oscillating form. At the post-lip of the stenosis the vortex intensity and shear stresses are found to be high due to the maximum pressure drop, where the fluid transit is slower, i.e. a prolonged staying time. This prolongation of staying time is potentially dangerous from the pathological point of view as this stagnation could be a factor in the genesis of thrombosis (blood clotting) in the post stenosis region.

Modelling accurately complex form of transitions of physiological blood flow in stenosis or heart deserves an accurate numerical approach. LES has the capability of modelling time-accurate transition to turbulent pulsatile flow, as demonstrated in the present article and also by Mittal *et al* [9], Scotti and Piomelli [8] and Liang and Papadakis [11]. Therefore, we believe that the researchers in this filed will benefit significantly from the LES approach.

The following limitations to the present study are acknowledged -

1. The stenosis in the model is simply placed eccentrically whereas pathological atherosclerotic stenoses are often complex as a form of concentric narrowing with eccentric and irregular elements.

2. For simplicity, a vessel of square cross-section has been studied in the present study unlike a biological vessel which is usually circular in cross-section.

3. The walls of the model are considered rigid unlike biological vessels which exhibit elasticity though loss of elasticity is a feature of arteriosclerosis.

4. Atherosclerosis most commonly affects vessel bifurcations while the model simply studies a single channel.

5. In-vivo flows in large arteries are spiral-laminar due to the twisting element imparted by the heart as it contracts around its own axis, see [20], but the flow studied is laminar pulsatile prior to the stenosis.

Further development of the computational code is required to overcome the above mentioned limitations and to study the post stenotic flow behaviour with physiological flow upstream of the stenosis in moderate to severe forms as well as at bifurcations, hence research is currently underway to investigate this using the LES.

Acknowledgements: The second author gratefully acknowledges the receipt of an ORS award and a studentship from the Faculty of Engineering. The authors thank to the anonymous reviewers for their valuable comments and suggestions on the earlier version of this paper, which have served to improve the manuscript.

References

[1] A. M. Makel, S. L. Alper, S. Izumo, Hemodynamic shear stress and its role in atherosclerosis, J. Ameriacn Medical Association (JAMA) 282 (1999) 2035–2042.

[2] A. Frydrychowicz, A. Harloff, B. Jung, M. Zaitsev, E. Weigang, T. A. Bley, M. Langer, J. Hennig, M. Markl, Time-resolved, 3-Dimensional Magnetic Resonance Flow Analysis at 3 T: Visualization of Normal and Pathological Aortic Vascular Hemodynamics, J. Comput. Assist Tomogr. 31(1) (2007) 9–15.

[3] M. D. Despande, D. P. Giddens, Turbulent measurement in a constricted tube, J. Fluid Mech. 97(1) (1980) 65–89.

[4] B. B. Lieber, D. P. Giddens, Post-stenotic core flow behavior in pulsatile flow and its effects on wall shear stress, J. Biomech. 23(6) (1990) 597–605.

[5] F. Ghalichi, X. Deng, A. D. Champlain, Y. Douville, M. King, R. Guidoin, Low Reynolds number turbulence modeling of blood flow in arterial stenosis, Biorheology 35(4-5) (1998) 281–294.

[6] T. S. Lee, W. Liao, H. T. Low, Numerical study of physiological turbulent flows through series arterial stenoses, Int. J. Numer. Meth. Fluids 46 (2004) 315–344.

[7] B. A. Younis, S. Spring, S. O. Neumann, B. Weigand, Simulation of flow in an exact replica of a diseased human carotid artery, Applied Math. Modelling 31 (2007) 2599–2609.

[8] A. Scotti, U. Piomelli, Turbulence models in pulsating flows, AIAA Journal 40(3) (2002) 537–544.

[9] R. Mittal, S. P. Simmons, H. S. Udaykumar, Application of large-eddy simulation to the study of pulsatile flow in a model arterial stenosis, J. Biomech. Eng. 123 (2001) 325–322.

[10] R. Mittal, S. P. Simmons, F. Najjar, Numerical study of pulsatile flow in a constricted channel, J. Fluid Mech. 485 (2003) 337–378.

[11] C. Liang, G. Papadakis, Large eddy simulation of pulsatile flow over a circular cylinder at subcritical Reynolds number, Comput. Fluids 36 (2007) 299–312.

[12] T. J. Pedley, High Reynolds number flow in tubes of complex geometry with application to wall shear stress in arteries, In:Biological Fluid Dynamics, Edited by Ellington C P and Pedley T J, Cambridge: The Company of Biologiests, Limited (1995) 219–241.

[13] T. J. Pedley, The fluid mechanics of large blood vessels, Cambridge University Press, 1980.

[14] Y. C. Fung, Biomechanics: Circulation, 2nd edition, Springer,1997.

[15] J. Smagorinsky, General circulation experiment with the primitive equations. i. the basic experiment, Monthly Weather Rev. 91 (1963) 99–164.

[16] U. Piomelli, J. Liu, Large-eddy simulation of rotating channel flows using a localized dynamic model, Phys. Fluids 7(4) (1995) 839–848.

[17] W. P. Jones, M. Wille, Large-eddy simulation of a plane jet in a cross-flow, Int. J. Heat and Fluid flow 17 (1996) 296–306.

[18] S. P. Sutera, M. H. Mehrjardi, Deformation and fragmentation of human red blood cells in turbulent flow, Biophysical J. 15 (1975) 1–10.

[19] D. L. Fry, Acute vascular endothelial changes associated with increased blood velocity gradients, Circulation Res. 22 (1968) 165–197.

[20] P. A. Stonebridge, C. M. Brophy, Spiral laminar flow in arteries?, The Lancet 338 (1991) 1360–1361.

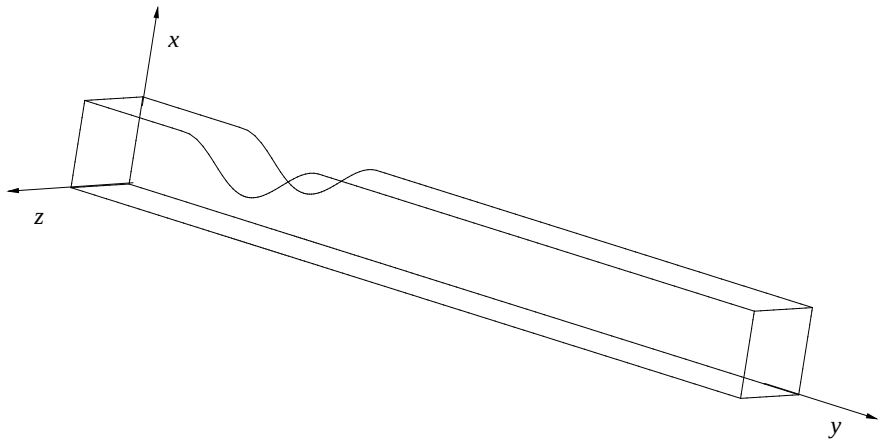

Figure 1: A schematic of the model of stenosis with the coordinate system.

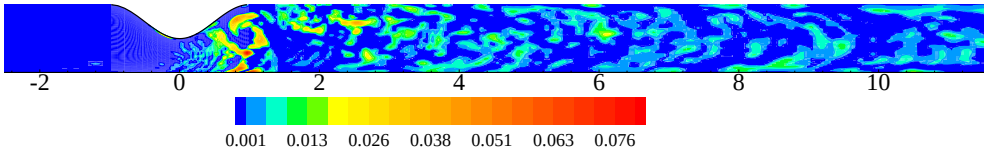

Figure 2: The results of the dynamic Smagorinsky constant.

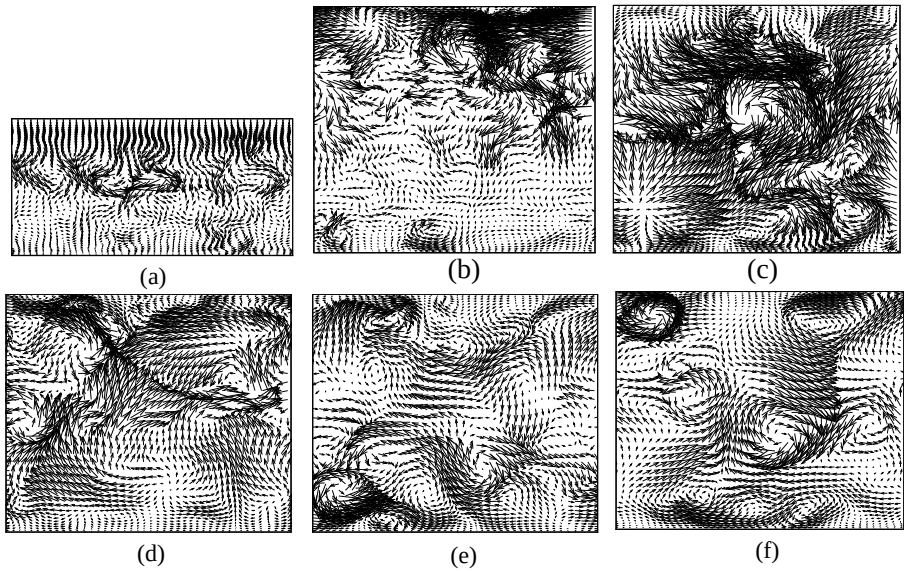

Figure 3: Velocity vectors plotted at (a) $y/L = 0$, (b) $y/L = 1$, (c) $y/L = 2$, (d) $y/L = 3$, (e) $y/L = 4$, and (f) $y/L = 5$.

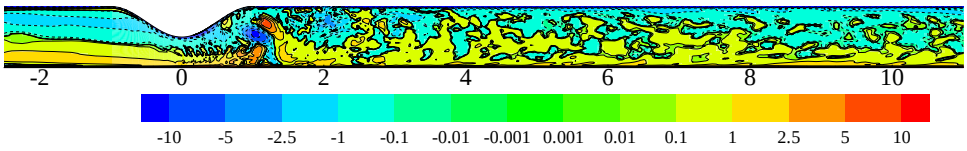

Figure 4: Spanwise average vorticity.

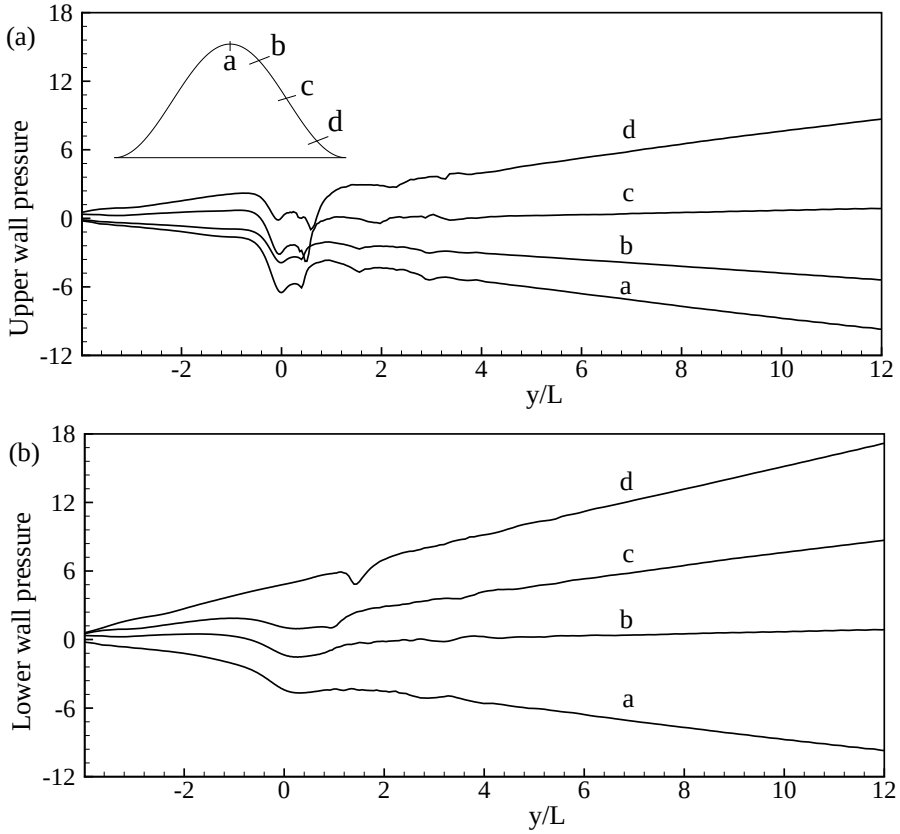

Figure 5: Instantaneous pressure at (a) the upper wall and (b) the lower wall.

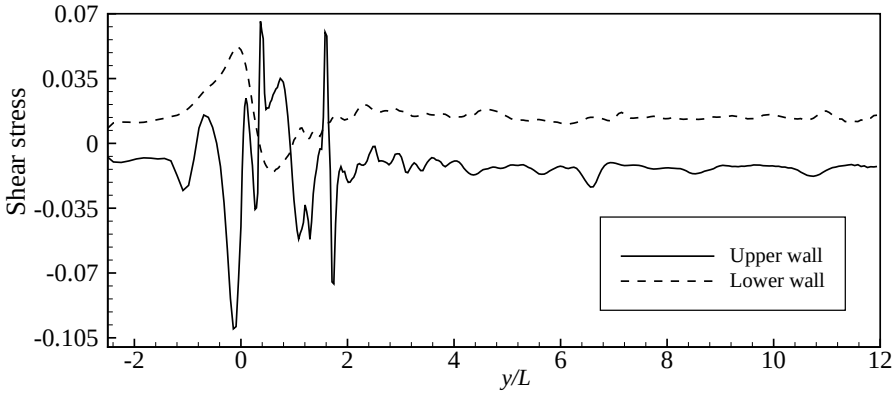

Figure 6: Instantaneous shear stresses at the upper and lower walls.

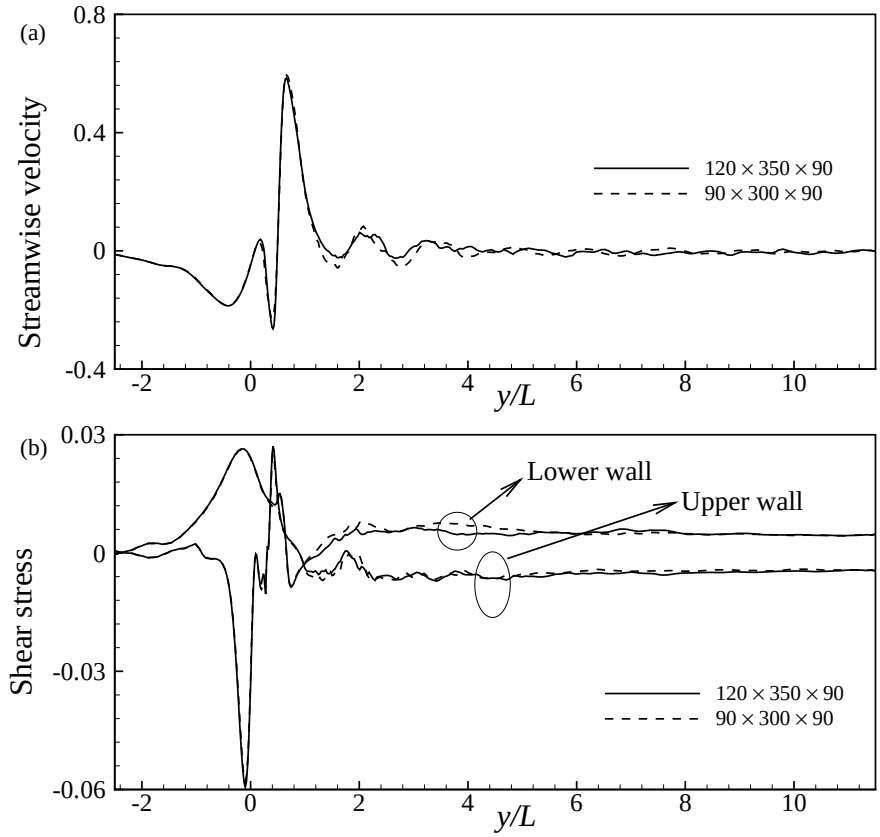

Figure 7: Grid independent test showing for the mean (a) centreline streamwise velocity and (b) shear stresses at the upper and lower walls.

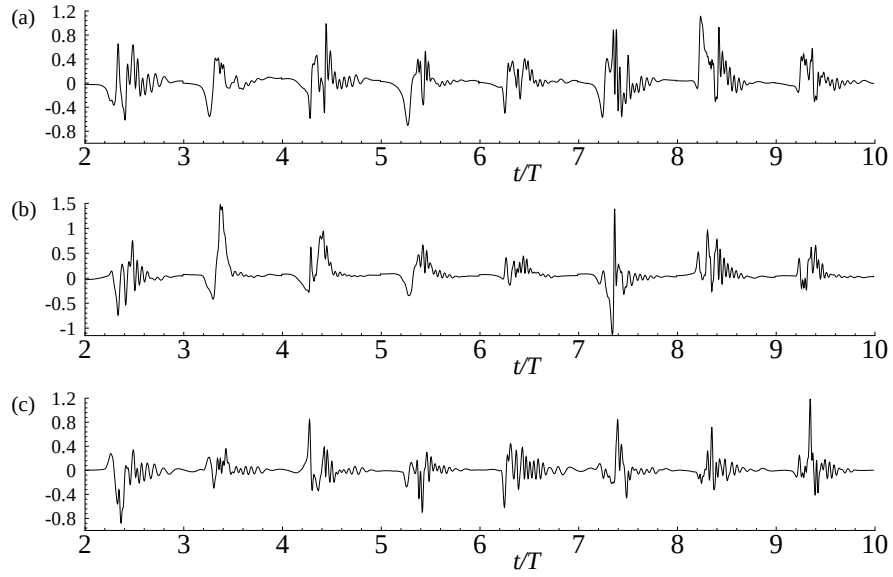

Figure 8: Velocity fluctuations with time; (a) $u''/\bar{V}$, (b) $v''/\bar{V}$, and (c) $w''/\bar{V}$, recorded at $y/L = 2.0$ in the centre.

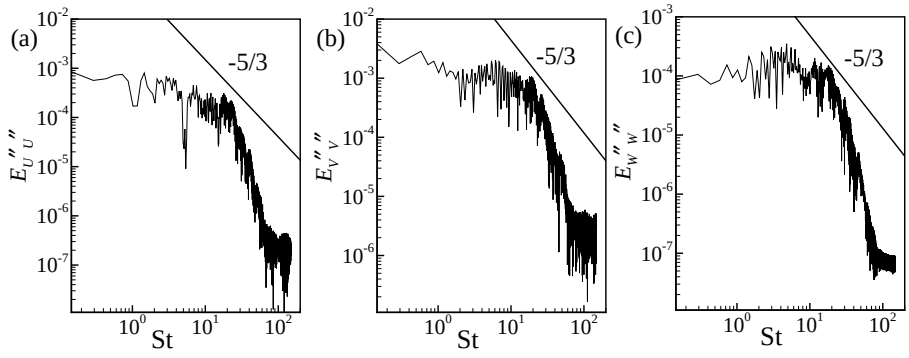

Figure 9: Energy spectrum for (a) u'', (b) v'' and (c) w''.